

## MECHANISM OF ADSORPTION OF WATER VAPOR BY MUSCOVITE: A MODEL BASED ON ADSORPTION CALORIMETRY

GAIKAT RAKHMATKARIEV\*

Institute of General and Inorganic Chemistry, Academy of Sciences of Uzbekistan, 77a, Kh. Abdullaev Ave.,  
700170 Tashkent, Uzbekistan

**Abstract**—Adsorption isotherms and differential heats of adsorption of water vapor by muscovite were measured at 303 K. The heats of adsorption are stepwise and each step corresponds to the stoichiometric formation of adsorption complexes of H<sub>2</sub>O molecules with K<sup>+</sup> ions, (H<sub>2</sub>O)<sub>n</sub>/K<sup>+</sup>, (*n* = 1–6), which are located on the basal and lateral (edge) faces. At saturation, the ditrigonal cavities of the basal faces are fully occupied by hexameric clusters. It is suggested that half of the K<sup>+</sup> ions on the basal faces come from neighboring layers by migration under the influence of the adsorbed H<sub>2</sub>O at the initial stage of adsorption. Similar migration of K<sup>+</sup> to the edges was also hypothesized, suggesting that only every second site can be occupied by a cluster. At the final stage of adsorption, H<sub>2</sub>O molecules are believed to form H-bonded bridges between the hexameric water/cation clusters on the basal faces, whereas on the edge faces no such effect is believed to occur. The mean molar integral adsorption entropy of water is ~–7 J/mol K less than the molar entropy of the bulk liquid. The mobility of H<sub>2</sub>O on muscovite is slightly less than in bulk water. Migration of K<sup>+</sup> cations under the influence of adsorbed H<sub>2</sub>O both on the basal and lateral faces of muscovite is reversible.

**Key Words**—Heats of Adsorption, Isotherm, Muscovite, Potassium Ion, Water Vapor.

### INTRODUCTION

Clays and other phyllosilicates are major sorbents for organic matter, contaminants and nutrients in soils. Water is the main means of transport by which these materials approach the adsorbent. Surface chemistry and features affecting water adsorption depend greatly on the crystallochemical properties of the minerals. This makes these materials very attractive for fundamental adsorption studies.

Muscovite is one of the most intensively studied phyllosilicates (Cantrell and Ewing, 2001; Diaz *et al.*, 2000; Pluijm *et al.*, 1988; Bracke *et al.*, 1995; White *et al.*, 1988; Zhang *et al.*, 1998 and Odelius *et al.*, 1997). The molecular structure of water layers adsorbed on micaceous minerals was studied by Sposito and Prost (1982) and Odelius *et al.* (1997). They found an ice-like structure of monolayer coverage based on (1) the longer-proton NMR relaxation time when compared to bulk liquid water, and (2) the potential of bulk water for an oriented growth with the hexagonal array of oxygen atoms on the basal surface of mica and 2:1 layer-type dioctahedral clay minerals. This conclusion has been supported by experimental and modeling studies by Sposito and Prost (1982), Odelius *et al.* (1997) and Miranda *et al.* (1998). However, Cheng *et al.* (2001), Swenson *et al.* (2000) and Bergman and Swenson (2000)

found that the hydration water in micaceous minerals is more disordered and more labile than a fully connected two-dimensional hydrogen-bond network, denoted as 2D ice. Cheng *et al.* (2001), using X-ray reflectivity, studied the structure of H<sub>2</sub>O adsorbed by muscovite mica under ambient conditions. They suggested a model where the first layer of adsorbed H<sub>2</sub>O molecules is at 1.3±0.2 Å above the mean position of a surface oxygen atom (O) and bound near the ditrigonal cavities on the mica surface. The next layer of H<sub>2</sub>O molecules forms at 2.5±0.2 Å above the surface O. The recent study by Park and Sposito (2002) presents Monte Carlo simulations of the structural properties of hydration H<sub>2</sub>O on muscovite. These data show an adsorbed layer of H<sub>2</sub>O molecules bound intimately to the ditrigonal cavities in the surface and additional H<sub>2</sub>O forming a hydrogen-bonded network where K<sup>+</sup> counterions may exist with hydrogen bonding to the surface O. These calculations also confirm the liquid-like hydration structure.

These studies showed that, in general, the water-density profiles vary across distances less than a few molecular diameters. This result indicates that the adsorbed H<sub>2</sub>O is limited to a few molecular layers. However, the molecular mechanism of H<sub>2</sub>O adsorption on muscovite is still unclear. In this study, quantitative data are presented to reveal a detailed hydration mechanism of muscovite at various levels of H<sub>2</sub>O adsorption by precision adsorption microcalorimetry. Among the precision structure-sensitive methods of investigation, adsorption calorimetry is unique (Akhmedov *et al.*, 1987; Dubinin *et al.*, 1989a, 1989b, 1989c; Boddenberg *et al.*, 1997, 1998, 2002, 2004), because it provides rich information about the surface,

\* E-mail address of corresponding author:  
gairat@chem.ccc.uz  
DOI: 10.1346/CCMN.2006.0540311

crystal chemistry, and the mechanism of ion-molecule cluster formation.

## MATERIALS AND METHODS

Muscovite is a mica phyllosilicate of ideal half unit-cell composition  $\text{KAl}_2(\text{Si}_3\text{Al})\text{O}_{10}(\text{OH})_2$ . The mica material, originating from the Aitik ore body (Sweden), was obtained from Boliden Mineral Ab. Muscovite crystals were handpicked from these materials with the aid of a microscope, ground in a pebble mill, and wet-sieved to  $<75 \mu\text{m}$ . A fraction  $<5 \mu\text{m}$  was then prepared using microsieves in an ultrasonic bath described by Hanumantha *et al.* (1995).

The X-ray diffraction (XRD) pattern of the sample was measured on a powder diffractometer using graphite-monochromatized  $\text{CuK}\alpha$  radiation by the step-scanning technique. The XRD pattern of the muscovite is shown in Figure 1. It reveals numerous basal reflections and the  $hkl$  reflections which are compatible with the  $2M_1$  polytype and with perfect ordering of the layers with respect to each other (JCPDS #06-0263).

Chemical analysis of the muscovite was carried out using a JY 70 type II ICP emission spectrometer. The chemical composition (wt.%) is:  $\text{SiO}_2$  45.33,  $\text{Al}_2\text{O}_3$  30.17,  $\text{Fe}_2\text{O}_3$  4.7,  $\text{MgO}$  1.26,  $\text{CaO}$  0.71,  $\text{Na}_2\text{O}$  0.6,  $\text{K}_2\text{O}$  10.01,  $\text{TiO}_2$  0.99 and loss on ignition 4.7. The chemical formula for half of a unit-cell was calculated on the basis of 22 positive and negative charges as follows:  $(\text{K}_{0.876}\text{Na}_{0.081}\text{Ca}_{0.052})_{\Sigma=1.009}(\text{Al}_{1.547}\text{Fe}_{0.243}^{3+}\text{Mg}_{0.129}\text{Ti}_{0.051})_{\Sigma=1.97}(\text{Si}_{3.108}\text{Al}_{0.892})\text{O}_{10}(\text{OH},\text{F})_2$ .

The muscovite powder was slightly compacted to pellets, which were subsequently crushed. Small pieces of this material, down to  $\sim 0.5 \text{ g}$ , were placed carefully in a 1 mm annular slit in contact with the wall of a cylindrical glass tube so that a sample of shallow-bed

configuration was obtained. For the initial dehydration, the material was heated under high vacuum at 423 K for 10 h.

Adsorption-calorimetric apparatus allows the adsorption isotherm and the heat of adsorption to be determined simultaneously and thus eliminates small errors associated with variability in the degassing procedure applied to the adsorbent. The adsorption isotherm was obtained by the volumetric method, on the basis of the difference between the amount of water introduced into the cell and amount of water vapor remaining in the dead space of the cell at equilibrium. The adsorbate was measured from a calibrated capillary, the level of liquid in which was measured with a KM-8 cathetometer with an accuracy of 0.005 mm.

Differential heats of adsorption were measured at 303 K with a differential microcalorimeter which was similar to the Tian-Calvet calorimeter (Calvet and Pratt, 1963), both with respect to the design and the method of measurement. A distinctive feature of Tian's methodology is the compensation method of measuring the heat flux, and the compensation heat flux is created directly in the working cell of the calorimeter with a large number of thermocouples using the Peltier endothermic effect. However, in the calorimeter used here, the compensation circuit of the thermopiles allows us to exclude Joule heating from the calculations. It was possible to linearize the dependence of the total compensation heat flux on the current strength in the chain of thermopiles. The Joule heating fluxes of different values from the two cells are mutually canceled (compensated), and the Peltier heat fluxes of the same value but of opposite sign are summed, *i.e.* the total compensation heat flux will be equal to the algebraic sum of the heat fluxes of both cells. Half of the heat flux from the working cell is reproduced or compensated in

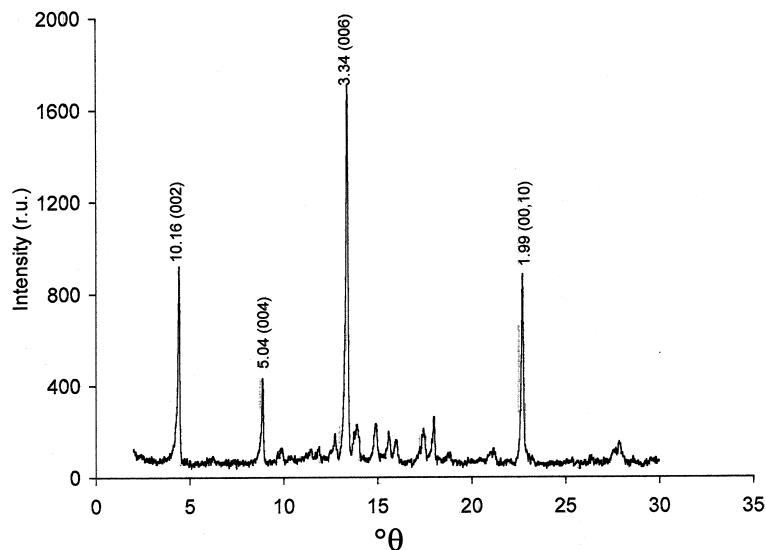


Figure 1. XRD pattern of muscovite used in this study (peak spacings in Å).

the blank of the calorimeter, and the other half of the heat flux of the working cell is compensated by the Peltier effect in the same cell, *i.e.* as in Tian-Calvet calorimeters, except in the latter, almost all of the heat effect is compensated by the opposite Peltier heat effect.

The heat liberated by the adsorption of an increment,  $\Delta a$  moles, of gas was determined by compensation of not less than 95% from the total heat flux by the Peltier effect with the precision of measurement of the current and the remaining 5% by integrating the area under the response curve generated by the thermopiles with a precision of  $\sim 3\%$ . This procedure allowed us to increase the accuracy of the heat flux measurement by  $\sim 10$  times. After each admission of a small amount of water,  $\Delta a$ , the heat flux was monitored until thermodynamic equilibrium was achieved. The attainment of this state is defined to be the time  $\tau$  at which the measured heat flux is just below the sensitivity of the instrument ( $1 \mu\text{W}$ ).

## RESULTS

Figure 2 shows the adsorption isotherm at 303 K of water ( $a$  in  $\mu\text{mol}_{\text{H}_2\text{O}}/\text{g}_{\text{MUSCOVITE}}$ ) on muscovite extending to  $\sim 10^{-6}$  of relative pressure  $p/p_0$  ( $p_0$  is the vapor

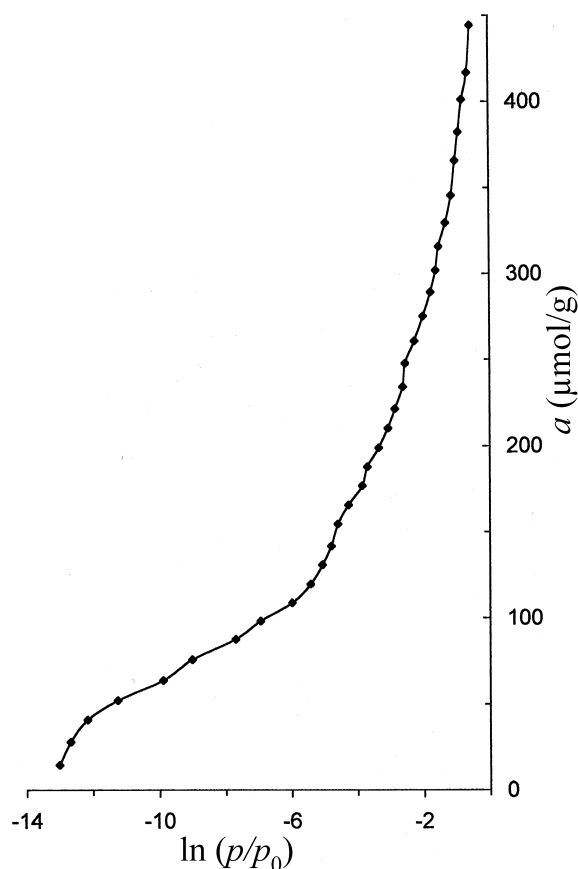


Figure 2. Adsorption isotherm of  $\text{H}_2\text{O}$  at 303 K on muscovite.  $p_0 = 4.24$  kPa is the vapor pressure of water at the temperature 303 K.

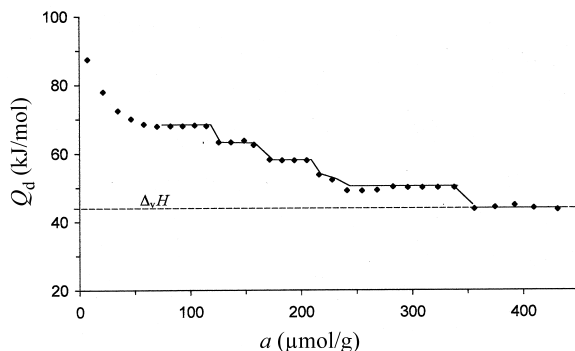


Figure 3. Differential heats of adsorption,  $Q_d$ , of  $\text{H}_2\text{O}$  at 303 K on the muscovite. The dashed line represents the heat of vaporization of bulk water at 303 K,  $\Delta_v H = 43.5$  kJ/mol.

pressure of water,  $p_0$  (303 K) = 4.24 kPa, *Handbook of Chemistry and Physics*, 1975). Starting with a convex shape, the adsorption isotherm increases monotonically to  $\sim 120 \mu\text{mol/g}$  and then increases steeply to  $\sim 450 \mu\text{mol/g}$ . With the BET plots being linear in the relative pressure range  $0.04 < p/p_0 < 0.25$ , the monolayer capacity  $a_m = 254 \mu\text{mol/g}$ , and the specific surface area  $S_{\text{H}_2\text{O}} = 21.5 \text{ m}^2/\text{g}$  (obtained by using the  $\text{H}_2\text{O}$  molecule cross-section  $\sigma_{\text{H}_2\text{O}} = 0.14 \text{ nm}^2$ ) were determined.

Figure 3 shows the differential heat of adsorption,  $Q_d$ , at 303 K of water for muscovite as a function of the amount adsorbed.  $Q_d$  starts at  $\sim 90$  kJ/mol and decreases to 68 kJ/mol at  $a = 68 \mu\text{mol/g}$ . The  $Q_d$  value remains constant at 68 kJ/mol and then decreases abruptly to  $a = 126 \mu\text{mol/g}$ , then again forms a plateau at 63.1 kJ/mol and drops again to 171  $\mu\text{mol/g}$ . Another plateau appears at 57.9 kJ/mol dropping to 216  $\mu\text{mol/g}$  with further increasing adsorption,  $Q_d$  dropping from 53.7 kJ/mol to 50 kJ/mol at 242  $\mu\text{mol/g}$ . The final steep drop in  $Q_d$  to the heat of vaporization ( $\Delta_v H = 43.5$  kJ/mol, dashed line) occurs after a plateau at 50 kJ/mol in the interval 242–358  $\mu\text{mol/g}$ . An additional 90  $\mu\text{mol/g}$  of water adsorbs with constant bonding energy 43.5 kJ/mol, which is equal to the heat of vaporization.

Figure 4 shows the time required for adsorption equilibrium ( $\tau$ ) as a function of water adsorption.

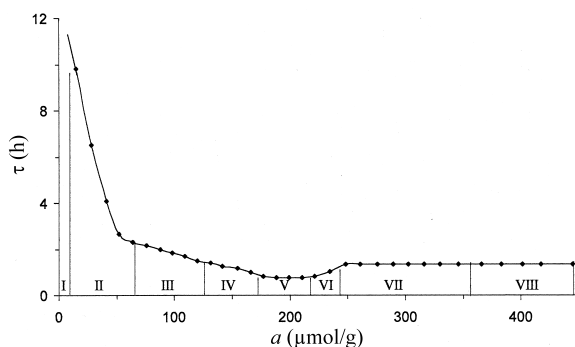


Figure 4. The time to establish adsorption equilibria,  $\tau$ , of  $\text{H}_2\text{O}$  at 303 K on muscovite.

Starting at 10 h, the curve decreases steeply to 2.6 h at  $a = 50 \mu\text{mol/g}$ , then drops slowly to 0.75 h at  $190 \mu\text{mol/g}$  and remains constant to  $a = 220 \mu\text{mol/g}$ . Finally,  $\tau$  increases to 1.33 h and remains constant. The indicated partitioning in sections I to VIII is considered below.

## DISCUSSION AND CONCLUSIONS

In the muscovite structure a sheet of octahedrally coordinated  $\text{Al}^{3+}$  ions is sandwiched between tetrahedral silicate sheets, with apical oxygen vertices pointing towards the octahedral sheet. The Si, Al tetrahedra are rotated within the basal plane. Aluminum is randomly substituted for Si with  $\text{Al}:\text{Si} = 1:3$ , and for charge compensation, K counterions are present at the center of all the hexagonal rings in the bulk. At the surface, half of the K ions remain after cleavage to preserve electro-neutrality. The positions and distribution of  $\text{K}^+$  were not experimentally redetermined.

Using  $\text{N}_2$  as a probe for the study of muscovite of the same origin, F. Villieras (unpublished data, 2003) found that the specific surface area is  $9 \text{ m}^2/\text{g}$  (BET method) and only half of the ditrigonal cavities on the basal faces contain  $\text{K}^+$  ions, which corresponds to  $22 \mu\text{mol/g}$ . In contrast, the present study of water adsorption on muscovite showed a specific area of  $21.5 \text{ m}^2/\text{g}$ . The width of the steps in the  $Q_d$  curve of  $\sim 45 \mu\text{mol/g}$  is twice as large as the value of  $\text{K}^+$  ions ( $22 \mu\text{mol/g}$ ) present on the basal faces. Additionally,  $13 \mu\text{mol/g}$  of  $\text{H}_2\text{O}$  are adsorbed with an energy greater than the energy of interaction of  $\text{H}_2\text{O}$  with  $\text{K}^+$  at the ditrigonal cavities of the basal faces. We assume that these extra sites are  $\text{K}^+$  ions at the edges of the (001) faces.

An idealized model of the muscovite structure and K cation distribution (Figure 5a) shows that at the surface, at least two types of sites might be detected. One site is disposed on the basal faces (ditrigonal cavities), the other type on the lateral faces (edges). These sites are denoted as  $S_d$  and  $S_e$ , and cations at these sites are denoted as  $\text{K}_d^+$  and  $\text{K}_e^+$ . Evidently, for the polar  $\text{H}_2\text{O}$  molecule,  $S_e$  is the more favorable site owing to the ion-dipole interaction with  $\text{K}^+$  because the degree of coordination produces an undersaturation of  $\text{K}^+$  ions, which decreases from  $S_e$  to  $S_d$ .

To establish a relationship between the number of  $S_d$  and  $S_e$  sites (Figure 5b), 45 basal units have been drawn in accordance with the number of ditrigonal cavities,  $45 \mu\text{mol/g}$ , and an equal number of double ditrigonal cavities. The side walls of these double ditrigonal cavities form the lateral faces. Forty-five such units form 24 sites,  $S_e$ . Half the number of the  $S_e$  sites (12) is very close to the experimentally determined value,  $13 \mu\text{mol/g}$ , which we attribute to  $\text{H}_2\text{O}$  adsorption with  $\text{K}^+$  ions at the  $S_e$  sites. Thus we can assume that only half of the possible sites,  $S_e$ , can be occupied by  $\text{H}_2\text{O}/\text{K}^+$  clusters. This restriction can be related to the relatively large lateral repulsive interaction between  $\text{H}_2\text{O}/\text{K}^+$

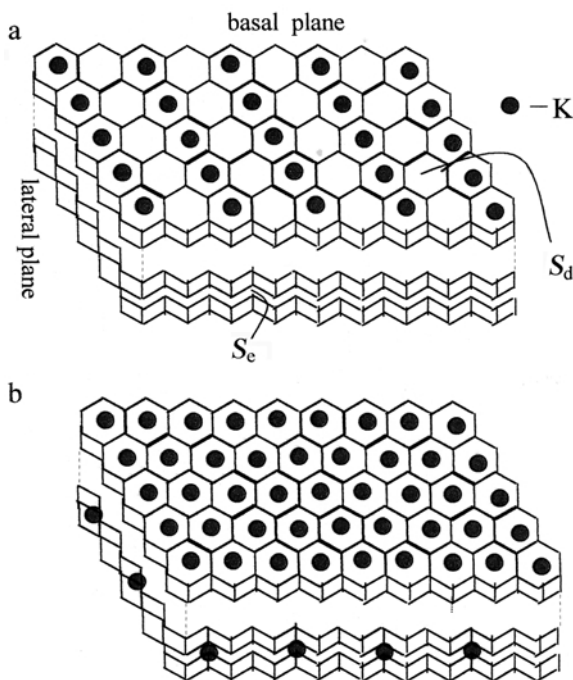


Figure 5. Idealized distribution of  $\text{K}^+$  cations onto the basal and lateral faces of muscovite before (a) and after (b) adsorption of  $\text{H}_2\text{O}$  molecules.

clusters on sites  $S_e$  and this may be the reason why the population of the adjacent positions is impossible.

The stepwise character of the heat of adsorption curve is considered to be related to the stoichiometric interaction of  $\text{H}_2\text{O}$  molecules with the undersaturated  $\text{K}^+$  cations on the basal and lateral faces. For a quantitative description of the hydration process, the calorimetric data set is divided into eight sections (Figure 6). The interpretation of the results is a model of the molecular picture. Section I corresponds to water adsorption on non-stoichiometric impurities and/or rehydroxylation of the surface with an energy of  $\sim 88 \text{ kJ/mol}$ . Section II corresponds to a stoichiometric interaction of  $\text{H}_2\text{O}$  molecules with  $\text{K}^+$  at the  $S_e$  sites ( $13 \mu\text{mol/g}$ ) and at the  $S_d$  sites ( $45 \mu\text{mol/g}$ ) with an energy varying from  $81.5$  to  $68 \text{ kJ/mol}$  to form  $\text{H}_2\text{O}/\text{K}^+$  ion-dipole clusters. At

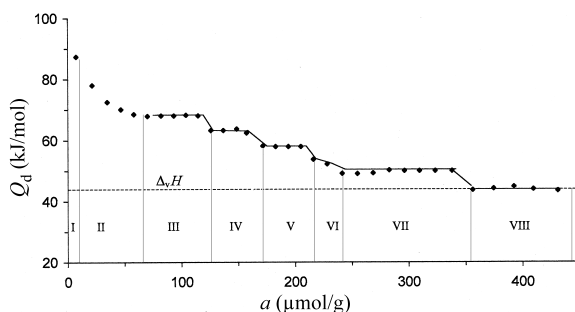


Figure 6. Differential heats of adsorption,  $Q_d$ , of  $\text{H}_2\text{O}$  at 303 K, on the muscovite. The calorimetric data set is arbitrarily divided into eight sections.

this stage of the adsorption process, all empty cavities on the basal faces and every second site on the lateral faces are filled with monomeric  $\text{H}_2\text{O}/\text{K}^+$  clusters and  $\text{K}^+$  ions are believed to migrate from neighboring layers (Figure 5b). Section III corresponds to the addition of one  $\text{H}_2\text{O}$  molecule to each of the initially formed clusters with constant binding energy of 68 kJ/mol, *i.e.* the formation of  $(\text{H}_2\text{O})_2/\text{K}^+$  clusters on the basal faces and edges. Sections IV and V correspond to formation of  $(\text{H}_2\text{O})_3/\text{K}_b^+$  clusters with an adsorption energy of 63.1 kJ/mol and  $(\text{H}_2\text{O})_4/\text{K}_b^+$  clusters with an adsorption energy of 57.9 kJ/mol on the basal faces. Section VI corresponds to further hydration of  $\text{K}^+$  on the edges to form  $(\text{H}_2\text{O})_3/\text{K}_c^+$  and  $(\text{H}_2\text{O})_4/\text{K}_c^+$  clusters with an adsorption energy varying from 53.7 to 50 kJ/mol. Section VII is related to the interaction of two  $\text{H}_2\text{O}$  molecules with a constant binding energy of 50 kJ/mol to the initially formed tetra-aqua complexes on the basal faces and edges and to the formation of pentameric and hexameric  $\text{H}_2\text{O}/\text{K}^+$  clusters. These six  $\text{H}_2\text{O}$  molecules completely shield the electrostatic field of the cation because the heats of adsorption up to the completion of adsorption at 448  $\mu\text{mol/g}$  do not differ from the heat of condensation (43.5 kJ/mol). Adsorption of an additional 90  $\mu\text{mol/g}$  of  $\text{H}_2\text{O}$  (section VIII) with heats equal to the heat of condensation, indicates that, on average, two  $\text{H}_2\text{O}$  molecules are added to each of the hexameric clusters already present on the basal faces. These hydrogen-bonded  $\text{H}_2\text{O}$  molecules are believed to form ‘bridges’ between the water/cation clusters on the basal faces exclusively. Clusters residing on the edges are too far apart from each other to be able to form H bonds with  $\text{H}_2\text{O}$ .

The experimentally obtained  $Q_d$  values, which are interpreted as  $\text{H}_2\text{O}$  on  $\text{K}^+$  ions of the different faces of muscovite, were compared with similar data that were obtained by Dzhighit *et al.* (1971) on synthetic KX and KY zeolites. These authors found that the heat of adsorption of water on  $\text{K}^+$  ions residing on crystallographic position SII (oxygen six-ring, similar to the configuration on the basal plane of muscovite) was equal to 65 kJ/mol (KY). However, the heat of adsorption of water on  $\text{K}^+$  at position SIII (oxygen four-ring) where a weak coordination of the  $\text{K}^+$  ions to framework oxygen atoms occurs, was equal to 80 kJ/mol (KX). These values are of similar magnitude to the case of initial  $\text{H}_2\text{O}$  adsorption on  $\text{K}^+$  ions on the basal and lateral faces of muscovite, respectively.

Figure 7 shows the differential adsorption entropies,  $\Delta S$ , at 303 K, of water adsorbed on the muscovite sample as a function of the amount adsorbed. The reported entropy values refer to the liquid state at the measuring temperature,  $\Delta \bar{S} = S_{\text{liq}} - \bar{S}$  where  $\bar{S}$  is the differential entropy of the adsorbed phase. Values of  $\Delta S$  were calculated from the corresponding measured heat data and the adsorption isotherm according to  $\Delta S = -(Q_d - \Delta vH/T - R\ln(p/p_0))$ .  $\Delta S$ , in accordance

with the stepwise nature of the heat curve, has multiple extremes. With the exception of the first, second, and eighth sections, the entire curve is below the level of the entropy of bulk water. The minimum corresponding to the formation of  $(\text{H}_2\text{O})_2/\text{K}^+$  clusters (section III of the  $Q_d$  curve) decreases to  $\sim -37$  J/mol K which is lower than the entropy of ice (at the entropy diagram,  $-26$  J/mol K). Then the entropy increases, going through several partial entropies corresponding to the successive additions of  $\text{H}_2\text{O}$  to the  $\text{K}^+$  cations. Molecules of  $\text{H}_2\text{O}$  increase their mobility, approaching a liquid-like state and even cross this level when H-bonding  $\text{H}_2\text{O}$  appears on the basal faces. The mean molar integral entropies are less ( $\sim 7$  kJ/mol K) than the entropy of the liquid. This result indicates that the mobility of  $\text{H}_2\text{O}$  in the clusters is slightly less than in bulk water. Our data confirm the liquid-like conditions of  $\text{H}_2\text{O}$  on the muscovite surface as proposed by Cheng *et al.* (2001).

The initial short equilibration time (Figure 4) is associated with the rearrangement of the  $\text{K}^+$  ions during the formation of the monomeric  $\text{H}_2\text{O}/\text{K}^+$  clusters on the basal and lateral faces. At  $\sim 50$   $\mu\text{mol/g}$  all vacant sites are fully occupied by  $\text{K}^+$  ions. Further adsorption by  $\text{K}^+$  ions initially present on the basal faces (22  $\mu\text{mol/g}$ ) occurs and therefore the equilibration time value is less, and equal to  $\sim 2.6$  h. On the curve, the change of the kinetics of adsorption is observed during the formation of  $\text{H}_2\text{O}/\text{K}^+$  clusters on the surface of muscovite. The water uptake occurs with a sequential increase of the relative pressure. The value  $\tau$  changes in a complex fashion with loading of  $\text{H}_2\text{O}$  to form tetra-aqua clusters on the basal and lateral planes (242  $\mu\text{mol/g}$ ). Subsequently,  $\tau$  settles at a value of  $\sim 1.33$  h.

To establish the rate of reversibility of the cation migration process, we studied the differential heats of  $\text{CO}_2$  adsorption on muscovite following a  $\text{H}_2\text{O}$  adsorption-desorption cycle. A linear quadrupole  $\text{CO}_2$  molecule might be expected to interact selectively with K cations. Whereas the absence of an ion-dipole interaction, as in the case of  $\text{H}_2\text{O}$ , occurs, the rather weak ion-quadrupole interaction with  $\text{CO}_2$  is not sufficient to extract cations

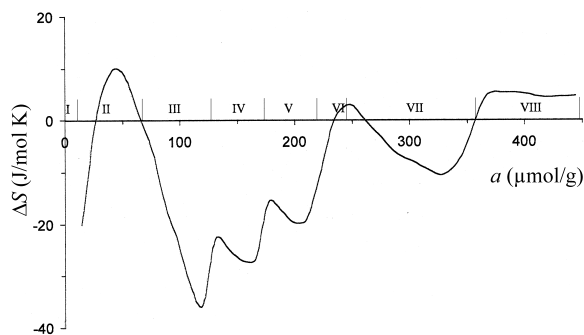


Figure 7. Differential entropy of adsorption,  $\Delta S$ , of  $\text{H}_2\text{O}$  at 303 K on muscovite. The entropy of the bulk liquid was taken as being equal to zero.

from the framework. The complete reversibility of migration is proven if the amount of  $K^+$  involving  $CO_2$  adsorption is initially,  $22 \mu\text{mol/g}$ .

The differential heats of  $CO_2$  adsorption initially form a plateau at  $a = 21 \mu\text{mol/g}$ .  $30 \text{ kJ/mol}$  corresponds to the energy of  $CO_2$  adsorption on  $K^+$ . This suggests that the number of  $CO_2/K^+$  complexes is equal to  $21 \mu\text{mol/g}$ . This value is nearly equivalent to the number of  $K^+$  on the surface of muscovite before  $H_2O$  adsorption. From these data we conclude that the migration of  $K^+$  ions on the basal and lateral faces under the influence of adsorbed  $H_2O$  of muscovite is fully reversible. A calorimetric investigation of the major thermodynamic adsorption functions and the molecular mechanisms of the adsorption of  $CO_2$  will be forthcoming.

#### ACKNOWLEDGMENTS

This work was performed under Project INTAS-2000, Ref. No: 00-505. The author is grateful to F. Villieras for providing the muscovite sample and for discussions and also to V. Choriev and D. Jumaeva for assistance with the calorimetric experiments.

#### REFERENCES

- Akhmedov, K.S., Rakhmatkariev, G.U., Dubinin, M.M. and Isirikyan, A.A. (1987) Heat of adsorption of methanol on the ultrahigh-silica zeolite silicalite. *Izvestiya Akademii Nauk SSSR, Seriya Khimicheskaya*, No. 8, 1717–1721.
- Bergman, R. and Swenson, J. (2000) Dynamics of supercooled water in confined geometry. *Nature (London)*, **403**, 283–286.
- Boddenberg, B., Rakhmatkariev, G.U. and Greth, R. (1997) Statistical thermodynamics of methanol and ethanol adsorption in zeolite NaZSM5. *Journal of Physical Chemistry, B*, **101**, 1634–1640.
- Boddenberg, B., Rakhmatkariev, G.U. and Viets, J. (1998) Thermodynamics and statistical mechanics of ammonia in Zeolite NaZSM5. *Berichtes Bunsenges Physical Chemistry*, **102**, 177–182.
- Boddenberg, B., Rakhmatkariev, G.U., Hufnagel, S. and Salimov, Z. (2002) A calorimetric and statistical mechanics study of water adsorption in zeolite NaY. *Physical Chemistry Chemical Physics*, **4**, 4172–4180.
- Boddenberg, B., Rakhmatkariev, G.U., Wozniak, A. and Hufnagel, S. (2004) A calorimetric and statistical mechanics study of ammonia adsorption in zeolite NaY. *Physical Chemistry Chemical Physics*, **6**, 2494–2501.
- Bracke, G., Satir, M. and Kraus, P. (1995) The cryptand [222] for exchanging cations of micas. *Clays and Clay Minerals*, **43**, 732–737.
- Calvet, E. and Pratt, H. (1963) *Recent Progress in Microcalorimetry*. Pergamon Press, Elmsford, New York.
- Cantrell, W. and Ewing, G.E. (2001) Thin film water on muscovite mica. *Journal of Physical Chemistry, B*, **105**, 5434–5439.
- Cheng, L., Fenter, P., Nagy, K.L., Schlegel, M.L. and Sturchio, N.C. (2001) Molecular-scale density oscillations in water adjacent to a mica surface. *Physical Review Letter*, **87**, 156103.
- Diaz, M., Farmer, V.C. and Prost, R. (2000) Characterization and assignment of far infrared absorption bands of  $K^+$  in muscovite. *Clays and Clay Minerals*, **48**, 433–438.
- Dubinin, M.M., Rakhmatkariev, G.U. and Isirikyan, A.A. (1989) Adsorption energy of water vapor on high-silica and pure-silica zeolites. *Izvestiya Akademii Nauk SSSR, Seriya Khimicheskaya*, No. 12, 2862–2864.
- Dubinin, M.M., Rakhmatkariev, G.U. and Isirikyan, A.A. (1989) Heat of adsorption of methanol and ethanol on high-silica zeolite ZSM-5. *Izvestiya Akademii Nauk SSSR, Seriya Khimicheskaya*, No. 11, 2633–2635.
- Dubinin, M.M., Rakhmatkariev, G.U. and Isirikyan, A.A. (1989) Heat of  $CO_2$  adsorption on high-silica zeolite ZSM5 and silicalite. *Izvestiya Akademii Nauk SSSR, Seriya Khimicheskaya*, No. 11, 2636–2638.
- Dzhigit, O.M., Kiselev, A.V., Mikos, K.N., Muttik, G.G. and Rakhmanova, T.A. (1971) Heats of adsorption of water vapour on X-Zeolites containing  $Li^+$ ,  $Na^+$ ,  $K^+$ ,  $Rb^+$  and  $Cs^+$  cations. *Transaction of the Faraday Society*, **67**, 458–467.
- Handbook of Chemistry and Physics*, 56<sup>th</sup> edition (1975) (R.C. Weast, editor). CRC Press, Cleveland, USA.
- Hanumantha Rao, K., Cases, J.M., Barres, O. and Forssberg, K.S.E. (1995) In: *Mineral Processing, Recent Advances and Future Trend* (S.P. Mehrotra and R. Shekhar, editors). Allied Publishers Limited, New Delhi, 29 pp.
- Miranda, P.B., Xu, L., Shen, Y.R. and Salmeron, M. (1998) Ice-like water monolayer adsorbed on mica at room temperature. *Physical Review Letter*, **81**, 5876–5879.
- Odelius, M., Bernasconi, M. and Parrinello, M. (1997) Two-dimensional ice adsorbed on mica surface. *Physical Review Letter*, **78**, 2855–2858.
- Park, S.-H. and Sposito, G. (2002) Structure of water adsorbed on a mica surface. *Physical Review Letter*, **89**, 085501-1–085501-3.
- Pluijm, B.A., Lee, J.H. and Peacor, D.R. (1988) Analytical electron microscopy and the problem of potassium diffusion. *Clays and Clay Minerals*, **36**, 498–504.
- Sposito, G. and Prost, R. (1982) Structure of water adsorbed on smectites. *Chemical Review*, **82**, 553–573.
- Swenson, J., Bergman, R. and Howells, W.S. (2000) Quasielastic neutron scattering of two-dimensional water in a vermiculite clay. *Journal of Chemical Physics*, **113**, 2873–2879.
- White, N.G. and Zelazny, L.W. (1988) Analysis and implications of the edge structure of dioctahedral phyllosilicates. *Clays and Clay Minerals*, **36**, 141–146.
- Zhang, Z.Z. and Bailey, G.W. (1998) Reactivity of basal surfaces, steps and edges of muscovite: AFM study. *Clays and Clay Minerals*, **46**, 290–300.

(Received 22 February 2005; revised 17 December 2005; Ms. 1018; A.E. David A. Laird)